Toxicology 488 (2023) 153471

Contents lists available at ScienceDirect

Toxicology

journal homepage: www.elsevier.com/locate/toxicol

A computational study on the biotransformation of alkenylbenzenes by a selection of CYPs: Reflections on their possible bioactivation

Lorenzo Pedroni [a], Jochem Louisse [b], Jean-Lou C.M. Dorne [c], Chiara Dall'Asta [a], Luca Dellafiora [a,*]

[a] Department of Food and Drug, University of Parma, Parma 43124, Italy
[b] Wageningen Food Safety Research, P.O. Box 230, 6700 AE Wageningen, the Netherlands
[c] European Food Safety Authority, Via Carlo Magno 1A, Parma 43124, Italy

ARTICLE INFO

Keywords:
Alkenylbenzenes
Apiol
Safrole
Dillapiol
Myristicin
Cytochrome P450
CYP1A1
CYP2A6
Molecular modeling
In silico toxicology

ABSTRACT

Alkenylbenzenes are aromatic compounds found in several vegetable foods that can cause genotoxicity upon bioactivation by members of the cytochrome P450 (CYP) family, forming 1′-hydroxy metabolites. These intermediates act as proximate carcinogens and can be further converted into reactive 1′-sulfooxy metabolites, which are the ultimate carcinogens responsible for genotoxicity. Safrole, a member of this class, has been banned as a food or feed additive in many countries based on its genotoxicity and carcinogenicity. However, it can still enter the food and feed chain. There is limited information about the toxicity of other alkenylbenzenes that may be present in safrole-containing foods, such as myristicin, apiole, and dillapiole. *In vitro* studies showed safrole as mainly bioactivated by CYP2A6 to form its proximate carcinogen, while for myristicin this is mainly done by CYP1A1. However, it is not known whether CYP1A1 and CYP2A6 can activate apiole and dillapiole. The present study uses an *in silico* pipeline to investigate this knowledge gap and determine whether CYP1A1 and CYP2A6 may play a role in the bioactivation of these alkenylbenzenes. The study found that the bioactivation of apiole and dillapiole by CYP1A1 and CYP2A6 is limited, possibly indicating that these compounds may have limited toxicity, while describing a possible role of CYP1A1 in the bioactivation of safrole. The study expands the current understanding of safrole toxicity and bioactivation and helps understand the mechanisms of CYPs involved in the bioactivation of alkenylbenzenes. This information is essential for a more informed analysis of alkenylbenzenes toxicity and risk assessment.

1. Introduction

Alkenylbenzenes are secondary metabolites of herbs and spices, like basil, fennel, and parsley to cite but a few, which are consumed worldwide as food per se, used as food and feed ingredients, as well as to extract essential oils widely used in food and feed (Eisenreich et al. 2021). Alkenylbenzenes are structurally related chemical analogues, including safrole, apiole, myristicin and dillapiole, sharing a 1,3-benzodioxole scaffold substituted by an allyl group at position 5 and various substitutions by methoxy groups on the aromatic ring (Fig. 1). Several members of this class proved marked toxicity to animals, including carcinogenicity, raising food safety concerns due to their occurrence in certain food and feed (Bampidis et al. 2021; Eisenreich et al. 2021; Groh et al. 2012). The carcinogenicity of alkenylbenzenes has a genotoxic mode of action through the cytochromes P450 (CYPs)-dependent formation of 1′-hydroxy metabolites (proximate carcinogens), which can subsequently be converted by phase II metabolism to 1′-sulfooxy metabolites (ultimate carcinogens) (Atkinson, 2018; Jeurissen et al. 2007). The ultimate carcinogens 1′-sulfooxy metabolites may form DNA adducts causing the genotoxic insult (Jeurissen et al. 2007). Hence, the genotoxicity of alkenylbenzenes inherently relies on the biotransformation to 1′-hydroxy metabolites, which is a key factor to investigate when studying their (geno)toxicity (Rietjens et al. 2005).

Safrole is one of the alkenylbenzenes for which a carcinogenicity study in rodents is available (Jin et al. 2011). Such data may be used to derive a point of departure (e.g. a BMDL10) that can be used to determine the margin of exposure (MOE; margin between BMDL10 and exposure estimate) in order to determine whether the chemical is a priority for risk management actions. Myristicin, apiol and dillapiole have stark structural analogies to safrole sharing the safrole 1,

* Corresponding author.
E-mail address: luca.dellafiora@unipr.it (L. Dellafiora).

https://doi.org/10.1016/j.tox.2023.153471
Received 25 January 2023; Received in revised form 23 February 2023; Accepted 27 February 2023
Available online 28 February 2023

3-benzodioxole scaffold along with the allylic side chain (Fig. 1) whose 1′-hydroxylation and subsequent 1′-sulfoxidation may produce the ultimate carcinogen metabolite. However, carcinogenicity studies on these compounds are still missing or inconclusive and toxicity data are generally scarce, although they have been described developmental toxicants, hepatotoxic, nephrotoxic and potentially able to reduce fertility (Dosoky and Setzer, 2021). They have been found at a variable level (from 0.2 % to 67.5 % of the total content of alkenylbenzenes, depending on the matrix) in essential oils mainly derived from nutmeg (myristicin), dill (dillapiole) and parsley (apiole) (Dosoky and Setzer, 2021). However, detected levels may vary based on environmental factors, which may influence their production by plants, and on the analytical methods used to perform the analysis (Gotz et al. 2022). Besides occurrence analysis, and germane to toxicity investigations to fill the current data gaps for risk assessment, the application of novel approach methodologies (NAMs), including in vitro and *in silico* methods, is considered preferred above generation of new in vivo data. An in vitro study has shown the following order of potency to form DNA adducts of these alkenylbenzenes in human HepG2 cells: safrole ≈ myristicin > dillapiole > apiole (Zhou et al. 2007). Concerning the bioactivation to proximate carcinogens, available in vitro evidence shows that safrole is solely bioactivated by CYP2A6 (Jeurissen et al. 2007), while myristicin is mainly bioactivated by CYP1A1, which has been also described as crucial for the myristicin-dependent formation of DNA adducts (Seneme et al. 2021; Zhu et al. 2019). However, neither the role of CYP1A1 to bioactivate safrole, nor of both CYPs to bioactivate apiole and dillapiole, or of CYP2A6 to bioactivate myristicin, have been duly assessed so far. This scenario provided a compelling rationale to further test CYP1A1 and CYP2A6 over other possible alkenylbenzenes as this incomplete picture may prevent those compounds from being properly evaluated for their toxicity and assessed for related risks.

The use of safrole as pure compound in food and feed production has been prohibited within both the EU and US due to its genotoxic and carcinogenic potential (Hausner and Poppenga, 2013; van den Berg et al. 2011). However, safrole may still be present in food and feed being part of essential oils and ingredients widely used in their production (Eisenreich et al. 2021). This makes still advisable to advance its toxicological understanding. In addition, safrole may co-occur along with other congeners (Eisenreich et al. 2021), including myristicin, apiole and dillapiole, suggesting the need for a broader assessment of safrole congeners – especially for those with strong structural similarities which may show analogies also from a toxicological standpoint. In such a process, toxicokinetic similarities including CYP-mediated formation of toxic metabolites should be addressed thoroughly while closely related members of a class are evaluated (More et al. 2019). Germane to this work's topic, the CYP-mediated formation of alkenylbenzenes proximate carcinogens may represent an upstream functional event to support such analysis. On this basis, safrole, apiole, dillapiole and myristicin have been assessed for their likeliness to act as substrates of CYP1A1 and CYP2A6, being those CYPs identified as crucial for the activation of the considered alkenylbenzenes (see above).

Based on the above, a previously validated *in silico* protocol (Dorne et al. 2022; Pedroni et al. 2023) has been applied to fill the current data gap for safrole, myristicin, apiol and dillapiole bioactivation. Of note, stand-alone *in silico* methods already proved to succeed in studying the toxicity of small molecules (e.g. (Qi et al. 2014; Rosell-Hidalgo et al. 2022; Vinken et al. 2021) to cite but a few) and molecular modelling approaches like that used here have already been applied to study the safety of chemicals (e.g. (Rosell-Hidalgo et al. 2022)). Specific applications of molecular modelling methodologies have a long story of use to study the CYP-mediated biotransformation of small molecules (Dorne et al. 2022; Itoh et al. 2010; Lewis et al. 1999; Pedroni et al. 2023; Sridhar et al. 2017). In this work, the interaction of safrole, apiole, dillapiole and myristicin with CYP1A1 and CYP2A6 has been investigated via docking and molecular dynamics simulations to assess the ligand-CYP complex stability over time as a mean to predict the substrate likeliness of those compounds, in agreement with previous studies (Dorne et al. 2022; Pedroni et al. 2023). Briefly, the geometries of interaction between the atoms undergoing the reaction (Fig. 1) and the Fe-heme have been monitored being a probing geometrical feature to discriminate CYP substrates from non-substrate molecules (Dorne et al. 2022). This approach already succeeded to study specifically the CYP-dependent bioactivation of safrole (Pedroni et al. 2023) and it has been applied here to extend the analysis over a set of safrole analogues possibly relevant to food safety.

Overall, this study investigated similarities and differences of bioactivation of safrole, apiole, dillapiole and myristicin by CYP1A1 and CYP2A6 being relevant to: i) extend the current understanding of safrole's congeners toxicity; ii) shed light on the mechanics of CYPs involved in such a process; and iii) to rationally design further dedicated investigations.

2. Experimental

2.1. Data source

The 3D structures of safrole, apiole, dillapiole and myristicin were retrieved in the .sdf format from the PubChem database (https://pubchem.ncbi.nlm.nih.gov) (Kim et al. 2021) with CID 8815, 10659, 10231 and 4276 respectively (CAS codes 140–67–0, 523–80–8, 484–31–1 and 607–91–0, respectively). The models of human CYP1A1 and CYP2A6 were derived from the crystallographic structures recorded in the Protein Data Bank (PDB; https://www.rcsb.org) (Berman et al. 2000) with PDB code 4I8V (Walsh et al. 2013) and 2PG6 (Sansen et al. 2007), respectively. The latter structure had two mutations, L240C and N297Q, which have been reverted to the wild-type sequence replacing the respective amino acid side chain using the Structure Editing/Rotamer tool of UCSF Chimera software (version 1.15) (Pettersen et al. 2004), in agreement with previous studies (Louisse et al. 2022).

2.2. Docking simulations

Docking simulations provided plausible binding architecture for the molecules under analysis within the catalytic site of the two CYPs. This was performed, in agreement with previous studies, using the GOLD software (version 2021) as it proved a high reliability to study protein–ligand interactions, including those with CYPs (Dellafiora et al. 2020; Dorne et al. 2022; Maldonado-Rojas and Olivero-Verbel, 2011).

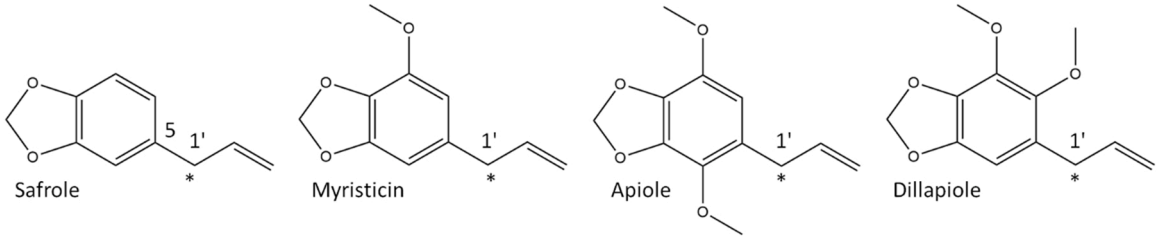

Fig. 1. Chemical structure of alkenylbenzenes under investigation. The asterisk indicates the atom undergoing the reaction.

The binding site was defined within a 10 Å radius sphere around the centroid of the substrate-binding site. The docking protocol was set according to previous studies setting ligands fully flexible and protein semi-flexible, allowing polar hydrogens to rotate freely (Dorne et al. 2022). The internal scoring function GOLDScore was used being optimised to predict ligand-binding positions as reported in the manufacturer declaration (https://www.ccdc.cam.ac.uk; accessed on 6th December 2022). The best scored pose for each ligand was further analysed through molecular dynamics (see below). In addition, the binding architecture of styrene as per PDB structure 4HGF – which has a structure closely related to that of alkenylbenzenes under analysis – has been used as a position restrain (constraint weight of 100 units) to facilitate the arrangement of ligands, in agreement with previous studies (Pedroni et al. 2022; Pedroni et al. 2023).

2.3. Molecular dynamics

Molecular dynamics allowed to assess the geometrical stability of CYP-ligand complexes over time as a mean to discriminate the likeliness of molecules under analysis to be substrates of CYP1A1 and CYP2A6. This was performed using GROMACS (version 2019.4) (Abraham et al. 2015), while ligands were parametrised with the CHARMM27 all-atom force field (Best et al. 2012). The hydrogen database was modified according to previous works (Dorne et al. 2022; Panneerselvam et al. 2015; Zhang et al. 2012) to parameterise the heme group. Input structures were solvated with SPCE waters in a cubic periodic boundary condition, and Na^+ and Cl^- were added as counter ions to neutralise the system. Prior to running simulations, each system was energetically minimised to avoid steric clashes and to correct improper geometries using the steepest descent algorithm with a maximum of 5000 steps. Subsequently, each system underwent isothermal (300 K, coupling time 2 psec) and isobaric (1 bar, coupling time 2 psec) 100 psec simulations before running 25 nsec simulations (300 K with a coupling time of 0.1 psec and 1 bar with a coupling time of 2.0 psec).

2.4. Statistical analysis

The statistical analysis of interatomic distances between the atom undergoing the reaction and the Fe atom of heme group has been done with SPSS IBM (v. 27.0, SPSS Inc., Chicago, IL, USA). For each complex, distance values of 5000 frames have been considered, expressed as means ± standard deviation (SD) and compared to each other using one-way ANOVA ($\alpha = 0.05$) with Bonferroni as post hoc test ($\alpha = 0.05$).

2.5. Cluster analysis of protein-ligand complexes trajectories

All the complexes were analysed to retrieve geometries of binding representative of the whole simulations, in agreement with previous studies (Del Favero et al. 2020). The GROMACS (version 2019.4) (Abraham et al. 2015) *cluster* command was used setting gromos as method and the cutoff at 0.2 nm.

3. Results and discussion

3.1. Fit-for-purpose validation

The procedure used here was validated in previous studies. Briefly, measuring the interatomic distance over time between the atom undergoing the reaction and the heme's Fe previously proved to be a probative geometrical parameter to predict the capability of small molecules, including safrole, to be biotransformed by CYPs (Dorne et al. 2022; Pedroni et al. 2023). Indeed, as previously demonstrated, the likeliness of a ligand to act as a substrate to form a certain metabolite (e.g. hydroxylated compounds) for a given CYP can be inferred when the atom undergoing the reaction is properly arranged to the heme's Fe by docking simulations and stably persists therein during molecular dynamics. In this respect, a distance threshold calculated as the average interatomic distance over time has been previously set at 0.53 nm to distinguish CYPs substrates (Dorne et al. 2022; Pedroni et al. 2023). On this basis and in order to provide a fit-for-purpose validation of the procedure for the case studies under analysis, myristicin and safrole were considered reference compounds. In fact, they are well-known substrates of CYP1A1 and CYP2A6, respectively, both forming 1′-hydroxy-metabolites (Jeurissen et al. 2007; Zhu et al. 2019). Concerning the arrangement of safrole and myristicin at the respective CYP's catalytic site provided by docking simulations, both compounds had the atom undergoing the reaction properly oriented toward the heme's Fe (Fig. 2A). Also, they both collected positive docking scores, pointing to their favourable interaction (the higher the score, the better the interaction (Dorne et al. 2022)) with the respective CYP (GOLDScore for safrole and myristicin of 162 and 172 units in CYP2A6, and CYP1A1, respectively; Table 1). Then, the distance between the atom undergoing the reaction and the heme's Fe was monitored over time through molecular dynamics. As shown in Fig. 2B, the atom undergoing the reaction of both safrole and myristicin was kept stably close to heme's Fe along all simulation with a mean distance of 0.39 ± 0.05 and 0.38 ± 0.04 nm for safrole within CYP2A6 and myristicin within CYP1A1, respectively. Of note, these distances were both below the threshold mentioned above and like those previously described for the atoms of substrates proven to undergo hydroxylation by CYPs (Dorne et al. 2022). This evidence eventually confirmed the reliability of the procedure used to the case studies under analysis.

3.2. Extended analysis of alkenylbenzenes interaction with CYP1A1 and CYP2A6

Once ascertained the procedural reliability, the interaction of dillapiole and apiole with CYP1A1 and CYP2A6, as well as that of safrole with CYP1A1 and myristicin with CYP2A6, was calculated to infer their respective likeliness to form 1′-hydroxy metabolites by the CYPs considered. Particularly, CYP1A1 was investigated since recent evidence proved its hepatic expression, suggesting to deeper study its role in xenobiotics clearance and possible bioactivation to genotoxic compounds (Lang et al. 2019). Moreover, CYP1A1 plays a pivotal role in myristicin 1′-hydroxylation as well as in myristicin-dependent DNA adducts formation, although other CYPs may have an ancillary role in its bioactivation (Zhou et al. 2007; Zhu et al. 2019). Therefore, the marked structural analogies between myristicin and the other alkenylbenzenes under analysis provided a sound rationale to test CYP1A1 against safrole, dillapiole and apiole. Adhering to this line of interpretation, CYP2A6, which is the sole described able to bioactivate safrole, has been tested against myristicin, apiol and dillapiole.

As shown in Table 1, all the alkenylbenzenes under analysis recorded positive and relatively high docking scores pointing to their theoretical capability to favourably interact with CYP1A1 and CYP2A6. However, the visual inspection of the docking poses revealed substantial differences in the way the various congeners docked at the catalytic site of CYP1A1 and CYP2A6 (Fig. 3). Concerning CYP2A6 (Fig. 3A), safrole properly oriented the atom undergoing the reaction to the heme's Fe (in line with its previously demonstrated biotransformation to 1′hydroxy-safrole, as described above) and a similar arrangement was observed for apiole and myristicin. Conversely, dillapiole showed a different architecture of binding with the atom undergoing the reaction arranged further away from the heme's Fe. Concerning CYP1A1 (Fig. 3B), as per safrole within CYP2A6, myristicin properly oriented the atom undergoing the reaction to the heme's Fe, in line with the previously described biotransformation to 1′-hydroxy-myristicin (see above). Conversely, the atom undergoing the reaction of apiol and dillapiole was displaced far from the heme's Fe. Surprisingly, the atom undergoing the reaction of safrole was found instead arranged close to the heme's Fe retracing the placement of that of myristicin, possibly suggesting its biotransformation to 1′-hydroxy-safrole by CYP1A1.

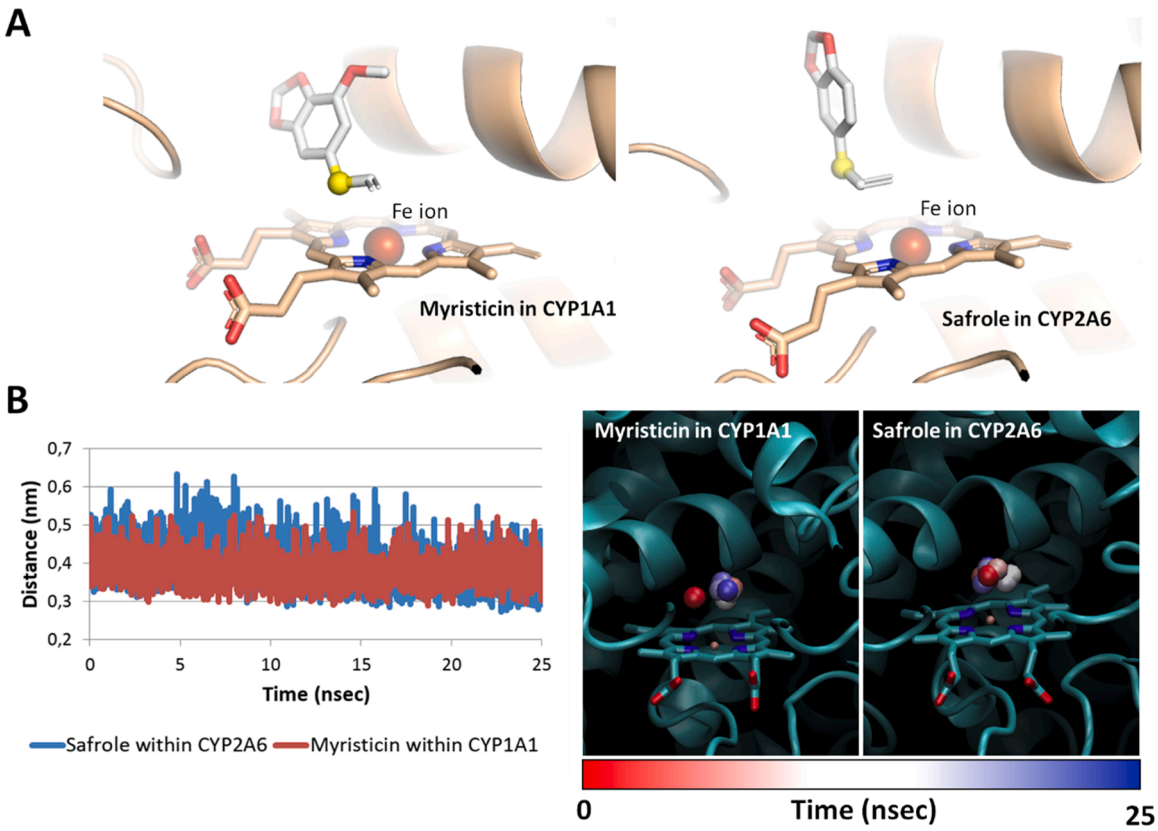

Fig. 2. Docking and molecular dynamics results for myristicin and safrole within CYP1A1 and CYP2A6, respectively. **A.** Docking pose of safrole and myristicin within CYP2A6 and CYP1A1, respectively. Ligands and heme group are represented in sticks while proteins are represented in cartoon. The heme's Fe atom is represented by red spheres. The atom undergoing the reaction is represented by yellow spheres. **B.** Molecular dynamics of safrole and myristicin within CYP2A6 and CYP1A1, respectively. The graph on the left shows the interatomic distances between heme's Fe and the atom undergoing reaction of myristicin and safrole within CYP1A1 and CYP2A6, respectively. The figure on the right shows the time step representation of the trajectories of atom undergoing reaction (shown in sphere) of myristicin within CYP1A1 and safrole within CYP2A6. Proteins are represented in cartoon, while heme is represented in sticks. The from-red-to-blue colour fade indicates the stepwise changes of coordinates along the simulation.

Table 1
Docking scores.

Compound	GOLDScore*	
	CYP1A1	CYP2A6
Safrole	168	162
Myristicin	172	148
Apiole	174	152
Dillapiole	179	158

Note: * a positive score indicates a favourable interaction with the protein, as per manufacturer declaration (https://www.ccdc.cam.ac.uk; accessed on 6th December 2022)

Each complex was then analysed through molecular dynamics to monitor whether the arrangement of the atom undergoing the reaction of the considered alkenylbenzenes to the heme's Fe was kept stable over time. As shown in Fig. 4, concerning the dynamics within CYP2A6, safrole was the sole of the alkenylbenzenes considered that properly arranged the atom undergoing the reaction close to the heme's Fe (with an average distance of 0.39 ± 0.05 nm, see above). Conversely, myristicin, apiole and dillapiole showed significantly higher distances compared to safrole, and all above the previously established cut-off of 0.53 nm (0.57 ± 0.07, 0.70 ± 0.07 and 0.65 ± 0.04 nm, respectively; $p < 0.001$). This suggests that the biotransformation to their respective 1′-hydroxy-metabolite may be less likely than that of safrole, considering previous evidence describing those distance ranges non-compliant to undergo an efficient hydroxylation by CYPs (Dorne et al. 2022; Pedroni et al. 2023). Concerning CYP1A1, dillapiole showed the highest mean distance between the atom undergoing the reaction and the heme's Fe (0.77 ± 0.05 nm) suggesting its biotransformation to 1′-hydroxy-dillapiole as not likely. Conversely, the atom undergoing the reaction of apiole approached the heme's Fe during the simulation (from around 10 nanoseconds onward) while being stable till the end of dynamics. Although the mean distance of 0.57 ± 0.17 nm, apiole might show a certain degree of 1′-hydroxylation by CYP1A1 based on the close interatomic proximity reached during the simulation. Surprisingly, the atom undergoing the reaction of safrole was kept close to the heme's Fe along the whole simulation (Fig. 4) and, though the mean interatomic distance was found statistically higher than that of myristicin (0.40 ± 0.04 and 0.38 ± 0.04; $p < 0.001$), it was compliant to those previously described as prone to undergo hydroxylation by CYPs (Dorne et al. 2022; Pedroni et al. 2023). A certain degree of safrole biotransformation to 1-'hydroxy-safrole by CYP1A1 shall be expected accordingly.

Based on the dynamics of interaction of safrole, myristicin, apiole and dillapiole, the latter two appeared to be those less likely prone to receive 1′-hydroxylation considering that the atom undergoing the reaction was not stably oriented toward the heme's Fe over time in neither of the two CYPs considered. However, apiole was considered prone of a limited 1′-hydroxylation by CYP1A1 as it properly arranged the atom undergoing the reaction to the heme's Fe during the simulation.

Taken together, the *in silico* results collected are in line with reported in vitro data on formation of the 1′-hydroxy-metabolites of safrole, myristicin and apiole, showing the highest catalytic efficiency for safrole 1′-hydroxylation (4.3 μL/min per mg microsomal protein) (Martati et al. 2012), followed by myristicin 1′-hydroxylation (0.73 μL/min per mg S9

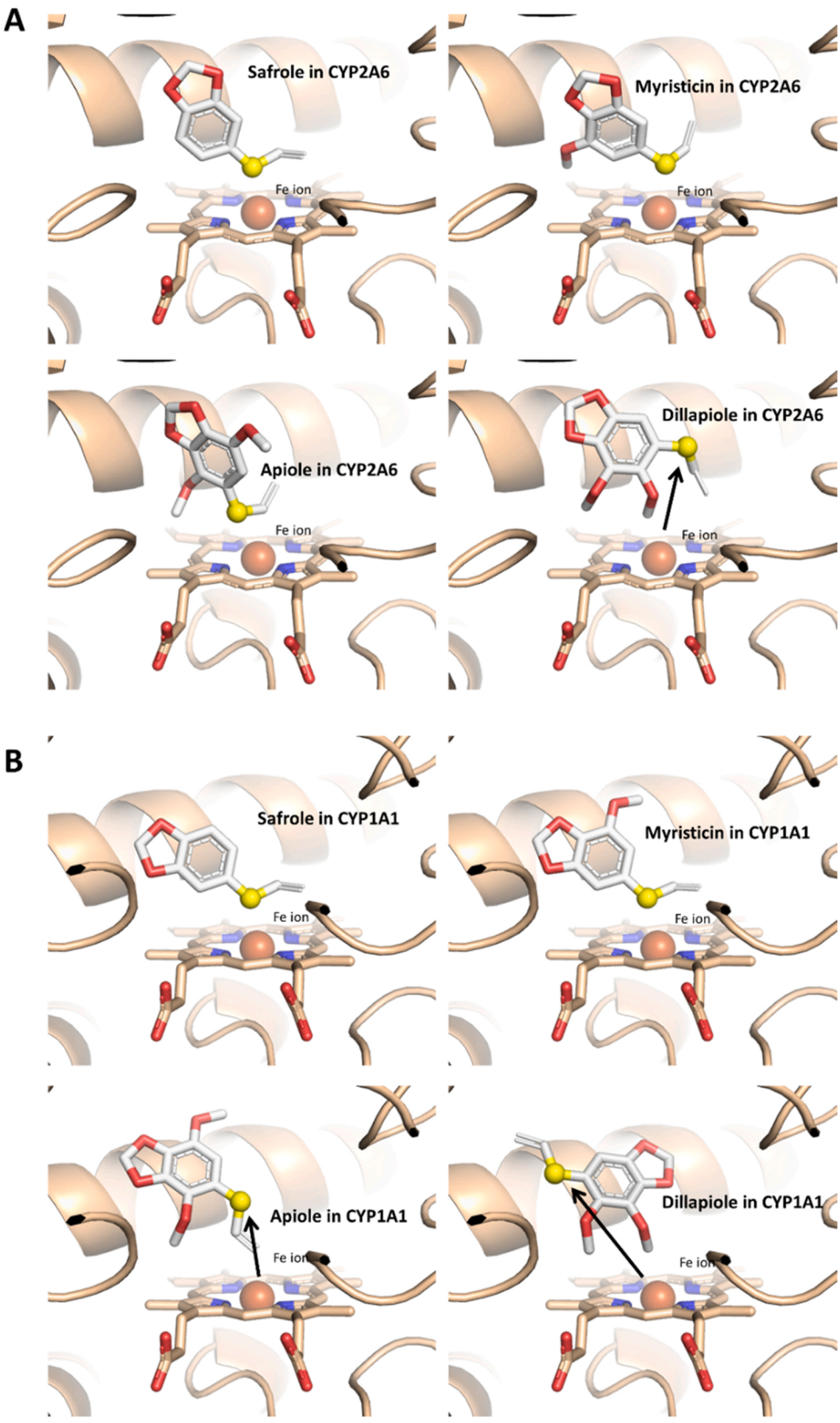

Fig. 3. Docking results for the alkenylbenzenes under investigation within CYP2A6 and CYP1A1. Ligands and heme group are represented in sticks while proteins are represented in cartoon. The heme's Fe atom is represented by red spheres. The atom undergoing the reaction is represented by yellow spheres. The black arrows indicate the displacement of the atom undergoing the reaction to the heme's Fe in certain complexes. **A.** Safrole, myristicin, apiole and dillapiole in CYP2A6. **B.** Safrole, myristicin, apiole and dillapiole in CYP1A1.

protein) (Al-Malahmeh et al. 2017), and the lowest efficiency for 1′-hydroxylation of apiol (0.34 μL/min per mg S9 protein) (Alajlouni et al. 2016). Based on the *in silico* results from the present study, one would expect an even lower efficiency of dillapiole 1′-hydroxylation, although it must be noted that possible bioactivation by CYPs other than CYP1A1 and CYP2A6 cannot be excluded. In this respect, the present work provided a mechanistic explanation for the available in vitro evidence detailing the incapability to properly arrange the atom undergoing the reaction to the heme's Fe as a basis for the lower efficiency in the bioactivation of myristicin, apiole and dillapiole compared to safrole,

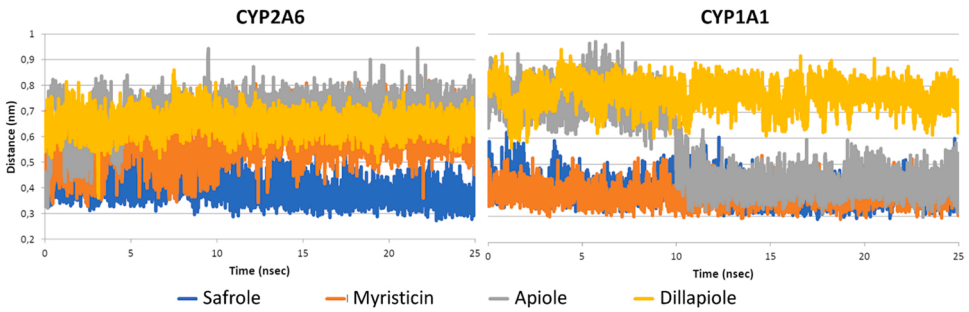

Fig. 4. Interatomic distances between the atom undergoing the reaction of safrole, myristicin, apiole and dillapiole to the heme's Fe within CYP2A6 or CYP1A1.

which is consistent with the lower toxicity of apiol and dillapiole described in vitro compared to safrole (Alajlouni et al. 2016; Zhou et al. 2007). Therefore, they may deserve a lower priority for future risk assessment evaluations. Although the final amount of ultimate carcinogens does not solely depend on the rate of formation of the proximate carcinogens, it is of interest to note that, in line with the *in silico* evaluation, the formation of DNA adducts in human HepG2 liver cells was more pronounced upon exposure to safrole and myristicin compared to apiole and dillapiole (Zhou et al. 2007).

Concerning myristicin, the results collected in this study are in line with the data available so far pointing out that it is preferentially 1′-hydroxylated by CYP1A1, although a certain degree of biotransformation by CYP2A6 can be expected as well. This is in line with previous evidence describing that other CYPs are involved in the bioactivation of myristicin, though with a lower efficiency compared to CYP1A1, and CYP2A6 could be counted in the list of CYPs bioactivating myristicin deserving further dedicated investigations (Zhou et al. 2007).

Concerning safrole, our data highlighted the mechanistic basis of its biotransformation by CYP2A6, showing the proper arrangement of the atom undergoing the reaction to the heme's Fe over the whole dynamic simulation. However, the present work also described that safrole could be efficiently 1′-hydroxylated by CYP1A1 showing a stable and proper arrangement of the atom undergoing the reaction to the heme's Fe. Of note, CYP1A1 has not been considered before as relevant for the biotransformation of safrole to 1′-hydroxy-safrole, though a certain degree of biotransformation was reported, but since its expression has been considered for long mainly extra-hepatic, its relevance for bioactivation of hepatoxicants has been thought limited (Ueng et al. 2004). However, recent studies demonstrated its inter-individual and high inducibility also in the liver, suggesting the need to reconsider the role of CYP1A1 in xenobiotics clearance and their bioactivation to genotoxic compounds (Lang et al. 2019). Moreover, although limited, previous evidence described the inducibility of CYP1A1 by safrole (Hu et al. 2007). These outcomes, along with the data reported in the present work, provided a compelling line of evidence pointing out the relevance to evaluate thoroughly the role of CYP1A1 in the biotransformation of safrole and congeners. This is critical to provide a sound background of knowledge to properly investigate the group of alkenylbenzenes from a risk assessment standpoint and eventually pointing out genotypes potentially with a high yield of formation of safrole's proximate carcinogen (e.g. when CYP1A1 is particularly expressed/induced in the liver).

4. Conclusions

Alkenylbenzenes include several genotoxic compounds that are bioactivated by CYPs to form 1′-hydroxy-metabolites, which act as proximate carcinogens that upon further sulfation form reactive metabolites that can damage DNA. However, for few alkenylbenzenes animal carcinogenicity data are available, hampering their inclusion in a risk assessment, as no margin of exposure (margin between BMDL10 of cancer study and estimated human exposure) can be determined. To fill these data gaps, application of NAMs is considered preferred above the performance of new in vivo animal studies, including *in silico* molecular dynamics studies as done in the present work. In this respect, this work addressed safrole, a well-known genotoxic alkenylbenzene for which a cancer study is available, and a series of poorly characterised structural analogues, i.e. apiole, dillapiole and myristicin. Our results described the low capability of apiole and dillapiole to being transformed into their 1′-hydroxy-metabolites by CYP1A1 and CYP2A6, in line with the limited in vitro kinetic and toxicity data available so far describing a lower efficiency of bioactivation (no data available for dillapiole) and limited DNA adducts formation compared to safrole. Taken together, these results may suggest that apiole and dillapiole are of lower concern for their toxicity, with a low priority in further risk assessment studies. In addition, safrole was shown in the present study as potentially being biotransformed to 1′-hydroxy-safrole by CYP1A1. Of note, CYP1A1 has been considered not relevant for safrole bioactivation as it was considered for long expressed mainly in extra-hepatic tissues. However, recent evidence has reported that CYP1A1 can be efficiently expressed and induced also in liver and safrole may act as an effective inducer. Taken together these data, along with the outcome collected in this work, point to the need of duly assessing CYP1A1 for its role in the formation of 1′-hydroxy-metabolites of safrole and other alkenylbenzenes to obtain more insights into the roles of different CYPs in their bioactivation.

As a general comment, analogies in the TK of compounds meant to be included in group assessment are pivotal for being actually grouped. Based on the differences described in this work, further analysis to better describe the CYPs involved in the bioactivation of alkenylbenzenes are advisable toward a more informed background for decision-making in that sense.

Regarding the use of NAMs in biotransformation studies, *in silico* 3D molecular modelling approaches, like the one presented here, already succeeded to study the biotransformation of small molecules by CYPs providing useful means to discriminate substrates from non-substrates (Dorne et al. 2022; Itoh et al. 2010; Pedroni et al. 2023). Therefore, 3D modelling may provide a self-standing and effective first-line analytical framework for the systematic analysis of CYP-related biotransformation. Assessing the role of specific CYPs in biotransformation reactions is useful to guide further dedicated in vitro investigations with respect to their full quantitative kinetic profiles (K_m and V_{max} of most relevant reactions), which are required input parameters for physiologically based kinetic (PBK) modelling.

Funding

The work was carried out as part of the EFSA (European Food Safety Authority) project "Data collection, update and further development of biologically-based models for humans and animal species to support transparency in food and feed safety" (OC/EFSA/SCER/2020/03). The view expressed in this article are the authors only and do not necessarily represent the views of the European Food Safety Authority.

Declaration of Competing Interest

The authors declare the following financial interests/personal relationships which may be considered as potential competing interests: Luca Dellafiora reports financial support was provided by European Food Safety Authority.

Data availability

Data will be made available on request.

Acknowledgments

This research benefits from the HPC (High Performance Computing) facility of the University of Parma, Italy.

References

Abraham, M.J., Murtola, T., Schulz, R., Páll, S., Smith, J.C., Hess, B., Lindahl, E., 2015. GROMACS: high performance molecular simulations through multi-level parallelism from laptops to supercomputers. SoftwareX 1–2, 19–25.

Al-Malahmeh, A.J., Al-Ajlouni, A., Wesseling, S., Soffers, A., Al-Subeihi, A., Kiwamoto, R., Vervoort, J., Rietjens, I., 2017. Physiologically based kinetic modeling of the bioactivation of myristicin. Arch. Toxicol. 91, 713–734.

Alajlouni, A.M., Al Malahmeh, A.J., Kiwamoto, R., Wesseling, S., Soffers, A., Al-Subeihi, A.A.A., Vervoort, J., Rietjens, I., 2016. Mode of action based risk assessment of the botanical food-borne alkenylbenzene apiol from parsley using physiologically based kinetic (PBK) modelling and read-across from safrole. Food Chem. Toxicol. 89, 138–150.

Atkinson, R.G., 2018. Phenylpropenes: occurrence, distribution, and biosynthesis in fruit. J. Agric. Food Chem. 66, 2259–2272.

Bampidis, V., Azimonti, G., Bastos, M.D., Christensen, H., Durjava, M.F., Kouba, M., Lopez-Alonso, M., Puente, S.L., Marcon, F., Mayo, B., Pechova, A., Petkova, M., Ramos, F., Sanz, Y., Villa, R.E., Woutersen, R., Brantom, P., Chesson, A., Westendorf, J., Manini, P., Pizzo, F., Dusemund, B., 2021. Safety and efficacy of a feed additive consisting of a tincture from the bark of Cinnamomum verum J. Presl (cinnamon tincture) for use in all animal species (FEFANA asbl). Efsa J. 19.

Berman, H.M., Westbrook, J., Feng, Z., Gilliland, G., Bhat, T.N., Weissig, H., Shindyalov, I.N., Bourne, P.E., 2000. The protein data bank. Nucleic Acids Res. 28, 235–242.

Best, R.B., Zhu, X., Shim, J., Lopes, P.E.M., Mittal, J., Feig, M., MacKerell, A.D., 2012. Optimization of the additive CHARMM all-atom protein force field targeting improved sampling of the backbone phi, psi and side-chain chi(1) and chi(2) dihedral angles. J. Chem. Theory Comput. 8, 3257–3273.

Del Favero, G., Mayer, R.M., Dellafiora, L., Janker, L., Niederstaetter, L., Dall'Asta, C., Gerner, C., Marko, D., 2020. Structural similarity with cholesterol reveals crucial insights into mechanisms sustaining the immunomodulatory activity of the mycotoxin alternariol. Cells 9.

Dellafiora, L., Oswald, I.P., Dorne, J.L., Galaverna, G., Battilani, P., Dall'Asta, C., 2020. An in silico structural approach to characterize human and rainbow trout estrogenicity of mycotoxins: proof of concept study using zearalenone and alternariol. Food Chem. 312.

Dorne, J., Cirlini, M., Louisse, J., Pedroni, L., Galaverna, G., Dellafiora, L., 2022. A computational understanding of inter-individual variability in CYP2D6 activity to investigate the impact of missense mutations on ochratoxin a metabolism. Toxins 14.

Dosoky, N.S., Setzer, W.N., 2021. Maternal reproductive toxicity of some essential oils and their constituents. Int. J. Mol. Sci. 22.

Eisenreich, A., Gotz, M.E., Sachse, B., Monien, B.H., Herrmann, K., Schafer, B., 2021. Alkenylbenzenes in foods: aspects impeding the evaluation of adverse health effects. Foods 10.

Gotz, M.E., Sachse, B., Schafer, B., Eisenreich, A., 2022. Myristicin and elemicin: potentially toxic alkenylbenzenes in food. Foods 11.

Groh, I.A.M., Cartus, A.T., Vallicotti, S., Kajzar, J., Merz, K.H., Schrenk, D., Esselen, M., 2012. Genotoxic potential of methyleugenol and selected methyleugenol metabolites in cultured Chinese hamster V79 cells. Food Funct. 3, 428–436.

Hausner, E., Poppenga, R.H., 2013. Hazards associated with the use of herbal and other natural Products. In: Peterson, M.E., Talcott, P.A. (Eds.), Small Anim. Toxicol. 335–356.

Hu, W.Y., Sorrentino, C., Denison, M.S., Kolaja, K., Fielden, M.R., 2007. Induction of Cyp1a1 is a nonspecific biomarker of aryl hydrocarbon receptor activation: results of large scale screening of pharmaceuticals and toxicants in vivo and in vitro. Mol. Pharmacol. 71, 1475–1486.

Itoh, T., Takemura, H., Shimoi, K., Yamamoto, K., 2010. A 3D model of CYP1B1 explains the dominant 4-hydroxylation of estradiol. J. Chem. Inf. Model. 50, 1173–1178.

Jeurissen, S.M.F., Punt, A., Boersma, M.G., Bogaards, J.J.P., Fiamegos, Y.C., Schilter, B., van Bladeren, P.J., Cnubben, N.H.P., Rietjens, I., 2007. Human cytochrome p450 enzyme specificity for the bioactivation of estragole and related alkenylbenzenes. Chem. Res. Toxicol. 20, 798–806.

Jin, M., Kijima, A., Suzuki, Y., Hibi, D., Inoue, T., Ishii, Y., Nohmi, T., Nishikawa, A., Ogawa, K., Umemura, T., 2011. Comprehensive toxicity study of safrole using a medium-term animal model with gpt delta rats. Toxicology 290, 312–321.

Kim, S., Chen, J., Cheng, T.J., Gindulyte, A., He, J., He, S.Q., Li, Q.L., Shoemaker, B.A., Thiessen, P.A., Yu, B., Zaslavsky, L., Zhang, J., Bolton, E.E., 2021. PubChem in 2021: new data content and improved web interfaces. Nucleic Acids Res. 49, D1388–D1395.

Lang, D., Radtke, M., Bairlein, M., 2019. Highly variable expression of CYP1A1 in human liver and impact on pharmacokinetics of riociguat and granisetron in humans. Chem. Res. Toxicol. 32, 1115–1122.

Lewis, D.F.V., Lake, B.G., George, S.G., Dickins, M., Eddershaw, P.J., Tarbit, M.H., Beresford, A.P., Goldfarb, P.S., Guengerich, F.P., 1999. Molecular modelling of CYP1 family enzymes CYP1A1, CYP1A2, CYP1A6 and CYP1B1 based on sequence homology with CYP102. Toxicology 139, 53–79.

Louisse, J., Dorne, J.L.C.M., Dellafiora, L., 2022. Investigating the interaction between organic anion transporter 1 and ochratoxin A: an in silico structural study to depict early molecular events of substrate recruitment and the impact of single point mutations. Toxicol. Lett. 355, 19–30.

Maldonado-Rojas, W., Olivero-Verbel, J., 2011. Potential interaction of natural dietary bioactive compounds with COX-2. J. Mol. Graph. Model. 30, 157–166.

Martati, E., Boersma, M.G., Spenkelink, A., Khadka, D.B., van Bladeren, P.J., Rietjens, I., Punt, A., 2012. Physiologically based biokinetic (PBBK) modeling of safrole bioactivation and detoxification in humans as compared with rats. Toxicol. Sci. 128, 301–316.

More, S.J., Hardy, A., Bampidis, V., Benford, D., Bennekou, S.H., Bragard, C., Boesten, J., Halldorsson, T.I., Hernandez-Jerez, A.F., Jeger, M.J., Knutsen, H.K., Koutsoumanis, K.P., Naegeli, H., Noteborn, H., Ockleford, C., Ricci, A., Rychen, G., Schlatter, J.R., Silano, V., Nielsen, S.S., Schrenk, D., Solecki, R., Turck, D., Younes, M., Benfenati, E., Castle, L., Cedergreen, N., Laskowski, R., Leblanc, J.C., Kortenkamp, A., Ragas, A., Posthuma, L., Svendsen, C., Testai, E., Dujardin, B., Kass, G.E.N., Manini, P., Jeddi, M.Z., Dorne, J., Hogstrand, C., Comm, E.S., 2019. Guidance on harmonised methodologies for human health, animal health and ecological risk assessment of combined exposure to multiple chemicals. Efsa J. 17.

Panneerselvam, S., Yesudhas, D., Durai, P., Anwar, M.A., Gosu, V., Choi, S., 2015. A combined molecular docking/dynamics approach to probe the binding mode of cancer drugs with cytochrome P450 3A4. Molecules 20, 14915–14935.

Pedroni, L., Dellafiora, L., Varra, M.O., Galaverna, G., Ghidini, S., 2022. In silico study on the Hepatitis E virus RNA Helicase and its inhibition by silvestrol, rocaglamide and other flavagline compounds. Sci. Rep. 12.

Pedroni, L., Louisse, J., Punt, A., Dorne, J.L.C.M., Dall'Asta, C., Dellafiora, L., 2023. A computational inter-species study on safrole phase I metabolism-dependent bioactivation: a mechanistic insight into the study of possible differences among species. Toxins 15, 94.

Pettersen, E.F., Goddard, T.D., Huang, C.C., Couch, G.S., Greenblatt, D.M., Meng, E.C., Ferrin, T.E., 2004. UCSF chimera - a visualization system for exploratory research and analysis. J. Comput. Chem. 25, 1605–1612.

Qi, Z., Miller, G.W., Voit, E.O., 2014. Rotenone and paraquat perturb dopamine metabolism: a computational analysis of pesticide toxicity. Toxicology 315, 92.

Rietjens, I., Boersma, M.G., van der Woude, H., Jeurissen, S.M.F., Schutte, M.E., Alink, G. M., 2005. Flavonoids and alkenylbenzenes: mechanisms of mutagenic action and carcinogenic risk. Mutat. Res. -Fundam. Mol. Mech. Mutagen. 574, 124–138.

Rosell-Hidalgo, A., Moore, A.L., Ghafourian, T., 2022. Prediction of drug-induced mitochondrial dysfunction using succinate-cytochrome c reductase activity, QSAR and molecular docking. Toxicology 28, 153412.

Sansen, S., Hsu, M.H., Stout, C.D., Johnson, E.F., 2007. Structural insight into the altered substrate specificity of human cytochrome P450 2A6 mutants. Arch. Biochem. Biophys. 464, 197–206.

Seneme, E.F., dos Santos, D.C., Silva, E.M.R., Franco, Y.E.M., Longato, G.B., 2021. Pharmacological and therapeutic potential of myristicin: a literature review. Molecules 26.

Sridhar, J., Goyal, N., Liu, J.W., Foroozesh, M., 2017. Review of ligand specificity factors for CYP1A subfamily enzymes from molecular modeling studies reported to-date. Molecules 22.

Ueng, Y.F., Hsieh, C.H., Don, M.J., Chi, C.W., Ho, L.K., 2004. Identification of the main human cytochrome P450 enzymes involved in safrole 1 '-hydroxylation. Chem. Res. Toxicol. 17, 1151–1156.

van den Berg, S., Serra-Majem, L., Coppens, P., Rietjens, I., 2011. Safety assessment of plant food supplements (PFS). Food Funct. 2, 760–768.

Vinken, M., Benfenati, E., Busquet, F., Castell, J., Clevert, D.A., de Kok, T.M., Dirven, H., Fritsche, E., Geris, L., Gozalbes, R., Hartung, T., Jennen, D., Jover, R., Kandarova, H., Kramer, N., Krul, C., Luechtefeld, T., Masereeuw, R., Roggen, E., Schaller, S., Vanhaecke, T., Yang, C., Piersma, A.H., 2021. Safer chemicals using less animals: kick-off of the European ONTOX project. Toxicology 458.

Walsh, A.A., Szklarz, G.D., Scott, E.E., 2013. Human cytochrome P450 1A1 structure and utility in understanding drug and xenobiotic metabolism. J. Biol. Chem. 288, 12932–12943.

Zhang, L., Silva, D.A., Yan, Y.J., Huang, X.H., 2012. Force field development for cofactors in the photosystem II. J. Comput. Chem. 33, 1969–1980.

Zhou, G.D., Moorthy, B., Bi, J., Donnelly, K.C., Randerath, K., 2007. DNA adducts from alkoxyallylbenzene herb and spice constituents in cultured human (HepG2) cells. Environ. Mol. Mutagen. 48, 715–721.

Zhu, X., Wang, Y.K., Yang, X.N., Xiao, X.R., Zhang, T., Yang, X.W., Qin, H.B., Li, F., 2019. Metabolic activation of myristicin and its role in cellular toxicity. J. Agric. Food Chem. 67, 4328–4336.